Journal of the Korean Society for Nondestructive Testing
Vol. 27, No. 3 (2007. 6)

Nondestructive Evaluation of Temporarily Repaired CFRP Laminates Subjected to Delaminations due to Localized Heating and Cyclic Loading Combined

Tae-Young Han* and Oh-Yang Kwon**,†

Abstract The reliability of cold-bonding repair technique of carbon-fiber reinforced plastics (CFRP) laminates, often used as a temporary repair for the airplane maintenance, has been evaluated during cyclic loading and localized heating by nondestructive methods. Major concern was given to the evolution of damage after repair in the form of delaminations due to localized heating and cyclic loading combined. An area of interest both on the specimen repaired by cold-bonding and the specimen without repair where delaminations were induced by localized heating and cyclic loading was monitored by acoustic emission (AE) testing and further examined by pitch-catch low-frequency bond testing, and pulse-echo high-frequency ultrasonic testing. The results showed that the reliability of cold-bonding repair would be significantly reduced by the localized heating and cyclic loading combined rather than by the cyclic loading only. AE monitoring appeared to be an effective and reliable tool to monitor the integrity of temporarily repaired CFRP laminates in terms of the structural health monitoring (SHM) philosophy.

Keywords: Cold-Bonding Repair, Delamination, Acoustic Emission, Pitch-Catch Low-Frequency Bond Testing, Pulse-Echo High-Frequency Ultrasonic Testing, Structural Health Monitoring

1. Introduction

CFRP composite structures are becoming widely used within the aerospace industry due to its superb specific strength and specific stiffness. However, they are also quite susceptible to various forms of damage. Common damage modes in CFRP laminates include matrix cracking, fiber breakage, and delamination (Matt, 2006). For composite laminates, the delamination is a major concern since this can significantly reduce the load carrying capacity of the laminate. Unlike metallic structures which are homogeneous, isotropic, and have the ability to dissipate energy through yielding, composite structures are relatively brittle and exhibit weak interlaminar strength due to their multi-layered structure, mechanical anisotropy and inhomogeneous composition (Kim et al, 2007). As a consequence, localized heating and cyclic loading combined (LHCLC) on CFRP composites can introduce delaminations that are not visible from the surface (Bolotin, 1996; MIL-HDBK-17, 1999).

The wide range of materials and configurations used in multi-layered structures and the need for nondestructive evaluation (NDE) of these laminates have resulted in the development of many different testing equipment and methods. Ultrasonic and acoustic testing methods have been quite successful. However, no single testing method has been found uniquely adequate to inspect and evaluate the wide variety of existing

Received: May 8 2007, Accepted: June 7, 2007. * Graduate School, Department of Mechanical Engineering, Inha University, ** Department of Mechanical Engineering, Inha University, 253 Yonghyun-dong, 402-751, Inchon, † Corresponding author: okwon@inha.ac.kr

applications in the field. Furthermore, the current NDE methods are often unreliable or impractical for the inspection of large-scale composite structures. Therefore, an SHM philosophy for monitoring of damage appears to be particularly well suited for aircraft structures comprised mainly of CFRP components (Hall and Conquest, 1999).

Awareness of inspection for the damage in composites should be included in the regular maintenance schedules for aircraft composite structures. Particular attention would be given to the areas more prone to damage. Repairs to civil aircraft structures are controlled and should be carried out according to an airplane structural repair manual (SRM). For other applications the repaired components would normally be expected to meet the original specification and mechanical performance requirements.

In order to operate airplanes economically, repair technology plays an important role, especially when the airframes are made of composite materials. Repairs can be classified as either temporary or permanent. Periodic maintenance repairs are mostly permanent repairs. Permanent repairs mean 'hot-bonding repair' requiring some elaborate arrangements in terms of curing equipments, inspection facilities, and patch materials. The repair also takes time to implement, whereas at a daily maintenance check, the damages to the airframes need quick repairs so that the airplane is ready to get in service promptly. Mostly these repairs are temporary repairs known as 'cold-bonding repair'. They need to be quick and effective, should not depend on availability of special equipment. When the cold-bonding repair is applied, however, the problem is that the temporarily repaired area must be repeatedly checked every inter-flight recess to ensure its integrity by either tap test or other NDE methods (Boeing SRM, 2007). Taking these reasons into consideration, it is necessary to monitor the soundness of the cold-bonding repair of composites using NDE methods.

During the AE testing, pattern recognition techniques (Matsuzaki and Todoroki, 2006) are employed to distinguish damage responses from noise signals due to benign changes such as temperature or loading variations (Marantidis et al, 1994; Kessler et al, 2001).

A large number of ultrasonic inspection methods exist for the monitoring of composite structures. Traditional ultrasonic NDE methods consist of generating and receiving bulk waves with conventional ultrasonic transducers either in a pulse-echo or a pitch-catch mode across the composites. The measured electrical impedance of transducers will be affected by the acoustic impedance of a specimen. The acoustic impedance of a composite laminate is altered by existing discontinuities, i.e. cracks, porosity, and delaminations. Therefore, these damages can easily be detected by analyzing changes in the reflected wave amplitude for normal incident pulse-echo ultrasonic testing (Teller et al, 1987). It is best for thin laminate structures to use a dual transducer with high center frequency to improve the near surface resolution and to eliminate the delay line multiples in composites. A dual-element transducer consists of two crystal elements housed in the same case, separated by an acoustic barrier. One element transmits longitudinal waves, and the other receives the reflected waves.

Although they are effective for delaminations and disbonds in small area, traditional high-frequency ultrasonic testing is generally ineffective for detecting damages in large area due to the coupling constraint between the structures and the transducer(s). In addition, it is impractical to use the pulse-echo technique in the air-coupled instrumentation (Fitch, 1991), which is an inevitable reason of why pitch-catch bond testing was employed in this experimental set-up. The pitch-catch bond testing utilizes low-frequency electronic sweep in the range of 20 to 40 kHz to activate the transmitting transducer and generate ultrasonic waves in the test sample.

The advantage of requiring no couplant allows the equipment's operator to contact a probe on the specimen and to locate the disbonds over the whole cyclic loading stage in spite of its vibration. A separate receiving transducer that holds a set distance from the transmitter picks up the waves propagated across the part. The ultrasound is carried in a plate wave mode across the structure between the two transducers. The transmitted waves are detected and a phase vs. amplitude display is used to show the effects of good and bad bonds on the sound path. Because the plate or Lamb waves (Worlton, 1961) are attenuated by coupling into the second layer in well-bonded laminates, signals will be small. In a disbond region the waves travel in the plate with very little attenuation or leakage into the backing material and a much larger signal pattern is displayed. Fig. 1 shows typical signals obtained by pitch-catch bond testing. The good bond signal will appear much smaller as in Fig. 1(a). Poor coupling into the part, such as transducer lift-off, results in the decreased amplitude or smaller size of the circular pattern as in Fig. 1 (b). The disbond signal, on the contrary, will be shown significantly larger and thus greatly reduces false readings as in Fig. 1 (c).

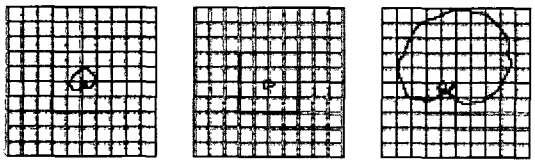

Fig. 1 Swept signal patterns in pitch-catch bond tester: (a) good bond signal (b) lift-off signal (c) disbond signal

Although the ultrasonic NDE methods described above for monitoring of composite structures are for local applications and cannot be implemented within an SHM strategy, in this study, the pitch-catch bond testing was carried out every five minutes during the whole cyclic loading stage to confirm the actual location where delaminations had occurred, and the pulse-echo ultrasonic testing was also carried out to locate the ply depth where delaminations had occurred after the completion of the cyclic loading to each specimen, i.e. the repaired specimen and the specimen without repair (BAC 5980, 2002).

2. Experiments

2.1 AE Sensor

Broadband piezoelectric transducers (B1025, Digital Wave) which show relatively flat response in the bandwidth between 100 kHz and 1.2 MHz were used in this experiment. The value of threshold is set to 45 dB to distinguish signals between the relevant and the irrelevant signals such as noise signals (Kessler, 2002). AE signals detected by the sensor were amplified by 40 dB via each preamplifier.

2.2 Ultrasonic Transducers

In order to get a very small focused beam diameter, a miniature tip dual transducer (MTD705, Panametrics), whose tip diameter is 5 mm and nominal element size is 3.8 mm, was employed in the pulse-echo high-frequency ultrasonic testing. A transducer of 10 MHz center frequency with a highly damped broadband response was selected to get the excellent time resolution and short wavelength for superior flaw resolution capabilities. For pitch-catch low-frequency bond testing, an air-coupled 40 kHz narrowband transducer (S-PC-P12L, Olympus) was adopted. The tip (spring-loaded) spacing of the transducer is 17 mm.

2.3 Specimen and Location of Sensors

Fig. 2 shows the geometry of the specimens with the location of AE sensors and the localized heat spot. Twelve plies of CFRP woven prepreg (Heatcon) were laid up by hand and autoclaved.

The directions for lay-up are shown in Fig. 3. Positioning AE sensors in equilateral triangle array was adopted to monitor and to confine the majority of received signals to those resulting from thermally stressed area under cyclic loading.

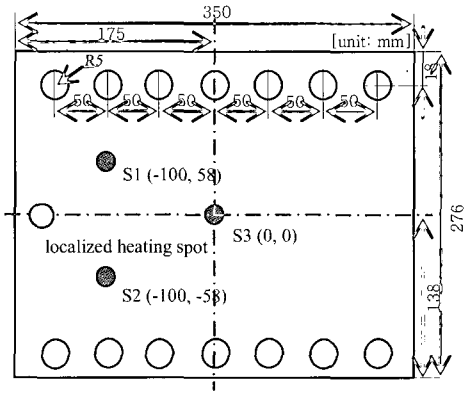

Fig. 2 Geometry of the specimen with equilateral triangle array of AE sensors and localized heating spot

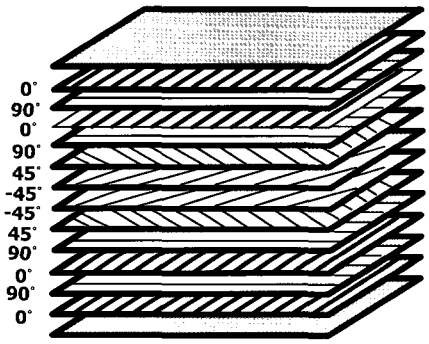

Fig. 3 Specimen lay-up

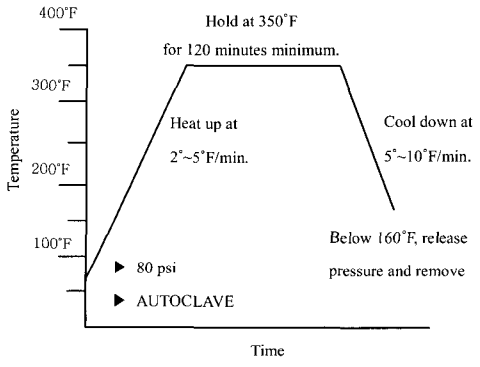

Fig. 4 Autoclave curing cycle

Fig. 4 shows the curing cycle for autoclave. The specimens were cured at 350°F for two hours under the pressure of 80 psi, which was kept until they were cooled down to 160°F (BAC 5578, 2002).

2.4 Reference Standard

A reference standard whose purpose is to calibrate the equipments prior to locating delamination and measuring ply depth was fabricated with the same processing as the specimen without repair (Galella, 2006). For simulated artificial defects, eleven pieces of Teflon tape (0.0041 mm thick) were inserted between every two adjacent plies. Fig. 5 and Fig. 6 show the location of each Teflon tape and its depth in the reference standard, respectively.

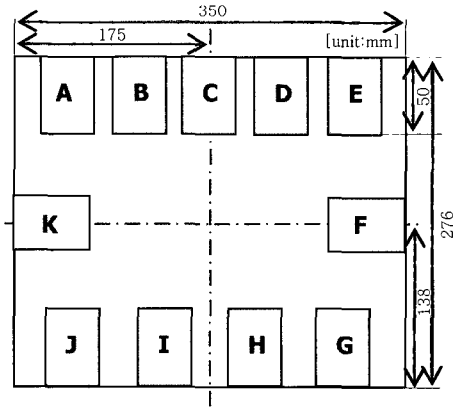

Fig. 5 Geometry of reference standard with locations of Teflon tapes

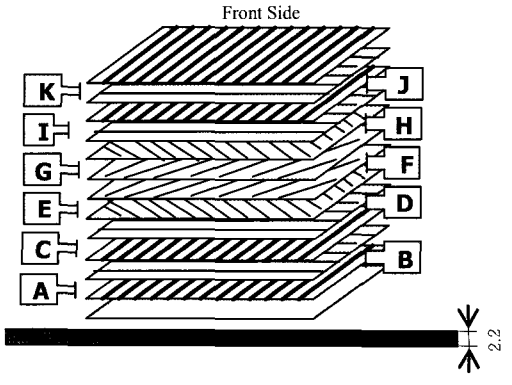

Fig. 6 Fabrication of reference standard

2.5 Experimental Setup

To acquire and monitor delamination signals from the specimens, an experimental setup as shown in Fig. 7 was prepared. It included an AE testing equipment (Mistras2001), a pitch-catch low-frequency bond tester (BondMaster), a pulse-echo high-frequency ultrasonic flaw detector (USN60), and an electro-hydraulic fatigue loading machine (Servopac-10). The minimum and the maximum load of cyclic loading were 10 kN and 50 kN, respectively, with a loading frequency of 5 Hz. The specimen was loaded symmetrically with respect to the specimen centerline. The system was also equipped with a heat-gun to apply localized heating to the specimen according to the temperature control plan: 1) the rise time (1 second to 60 seconds): 77 °F to 300 ± 15 °F, 2) the duration (61 seconds to 300 seconds): 301 °F to 340 ± 15 °F, and 3) the decline time (without heating, 301 seconds to 360 seconds): 340 °F to 95 ± 15 °F. While the cyclic loading was continuously applied to the specimens, the localized heating to the specimen was applied at eight different stages. In order to have the heat-flow focused onto the specimen, a focusing tube with inner diameter (exit side) of 15 mm was attached to the heat-gun. Table 1 shows the experimental cycle conditions in the experiments.

Table 1 Experimental cycle conditions

Specimen \ Cycle		Cyclic loading			Localized heating		
	Stage	minute	cycle	Load [kgf/㎠]	minute	cycle	Temperature [°F]
Specimen Without Repair	0	240	1~72,000	1,000/5,000	No heat application		
	1st	30	72,001~81,000	1,000/5,000	5	79,500~81,000	77~340±15 °F
	2nd	30	81,001~90,000	1,000/5,000	5	88,500~90,000	77~340±15 °F
	3rd	30	90,001~99,000	1,000/5,000	5	97,500~99,000	77~340±15 °F
	4th	30	99,001~108,000	1,000/5,000	5	106,500~108,000	77~340±15 °F
	5th	30	108,001~127,000	1,000/5,000	5	115,500~127,000	77~340±15 °F
	6th	30	127,001~136,000	1,000/5,000	5	134,500~136,000	77~340±15 °F
	7th	30	136,001~144,000	1,000/5,000	5	143,500~144,000	77~340±15 °F
	8th	30	144,001~153,000	1,000/5,000	5	151,500~153,000	77~340±15 °F
	Total	480	153,000		40	12,000	
Repaired specimen	0	240	1~72,000	1,000/5,000	No heat application		
	1st	30	72,001~81,000	1,000/5,000	5	79,500~81,000	77~340±15 °F
	2nd	30	81,001~90,000	1,000/5,000	5	88,500~90,000	77~340±15 °F
	3rd	30	90,001~99,000	1,000/5,000	5	97,500~99,000	77~340±15 °F
	4th	30	99,001~108,000	1,000/5,000	5	106,500~108,000	77~340±15 °F
	5th	30	108,001~127,000	1,000/5,000	5	115,500~127,000	77~340±15 °F
	6th	30	127,001~136,000	1,000/5,000	5	134,500~136,000	77~340±15 °F
	7th	30	136,001~144,000	1,000/5,000	5	143,500~144,000	77~340±15 °F
	8th	30	144,001~153,000	1,000/5,000	5	151,500~153,000	77~340±15 °F
	Total	480	153,000		40	12,000	

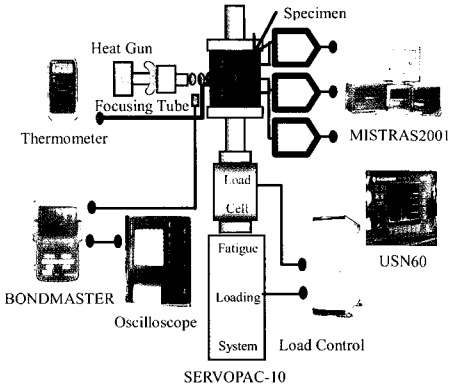

Fig. 7 A schematic of experimental setup

2.6 Monitoring Setup

For AE monitoring of the specimen during the cyclic loading and localized heating, a software feature for source location in the Mistras2001 was utilized. During the whole cyclic loading, the pitch-catch low-frequency bond testing using the BondMaster connected to an oscilloscope was performed every five minutes to identify and to locate where delaminations had occurred. Finally, the pulse-echo high-frequency ultrasonic testing was conducted after final stage of each repaired specimen and also for the specimen without repair. Besides the analysis of various signals from the above mentioned three NDE methods, scanning electron microscopy (SEM) was also carried out.

2.7 Repair Methods of CFRP

Fig. 8 and Fig. 9 show the cure cycle of hot-bonding and cold-bonding, respectively. The thick solid lines in Fig. 9 mean the total curing time required to cure the local area of the specimen at 150°F. The lower line in X-axis represents the initial curing time of 25 minutes and the upper line in X-axis indicates the full curing time of 40 minutes. Table 2 shows comparable information of repair conditions for hot-bonding and cold-bonding. As shown in the table, the hot-bonding process needs more complicated setup and takes much more time compared to the cold-bonding process. Fig. 10 illustrates the lay-up method of composite laminates to a cut-out area to be repaired. The cut-out area is tapered and overlapped by plies.

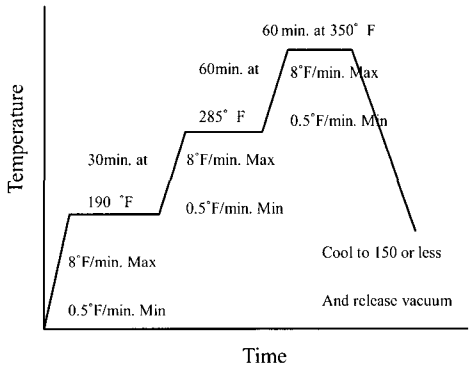

Fig. 8 Hot-bonding curing cycle

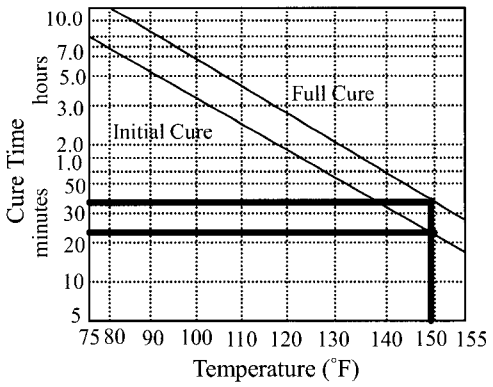

Fig. 9 Cold-bonding curing cycle

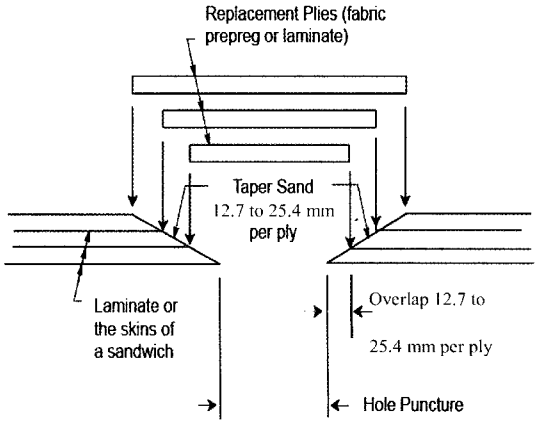

Fig. 10 Details of the laminates repair geometry

Fig. 11(a) and (b) represents photographs before and after repair. The cut-out and repair completion shown in the left-hand side belong to the cold-bonding repair and those shown in the right-hand side belong to the hot-bonding repair (BAC 5337, 2000).

Table 2 Comparable information of the two repair methods

	Hot-bonding	Cold-bonding
Equipment	HEATCON 9200	Wet Lay-up
Material	Woven Prepreg	Woven Dry Fabric
Adhesive	Prepreg	Resin Compound
Cure Temp.	Max. 350°F	Max. 150°F
Cure Time	200 minutes	75 minutes
Pressure	40±2 psi	20±2 psi

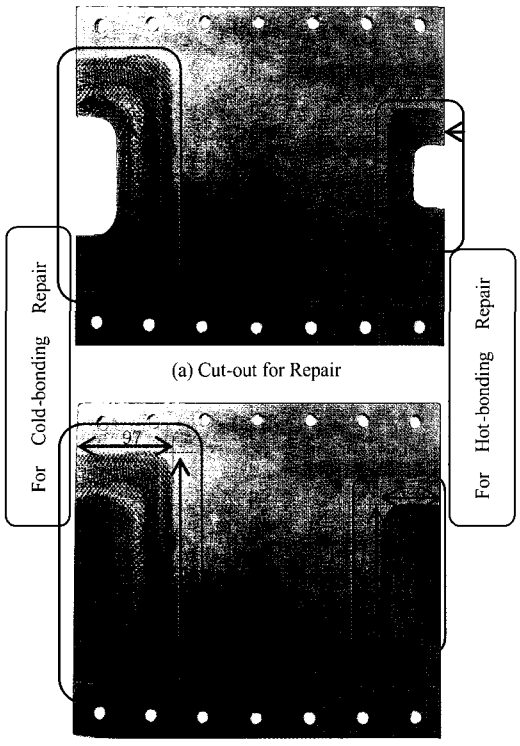

(a) Cut-out for Repair

(b) Completion

Fig. 11 Specimens repaired by cold-bonding and hot-bonding

3. Results and Discussion

The correlations among data resulted from each NDE method including SEM micrographs are analyzed in this section. After completing each experiment in the repaired specimen and the specimen without repair, specific data sets including amplitude profile of delaminations (APD) by the pitch-catch low-frequency bond testing and depth profile of delaminations (DPD) by pulse-echo high-frequency ultrasonic testing are obtained. Each result clearly presents comparable information of the specimen under two mechanical stresses, i.e. (1) LHCLC where localized heating was applied at the left side close to the edge of the specimen and (2) cyclic loading only (CLO) that is covered with the whole area except for the localized heating. Fig. 12 shows the APD obtained from both the repaired specimen and the specimen

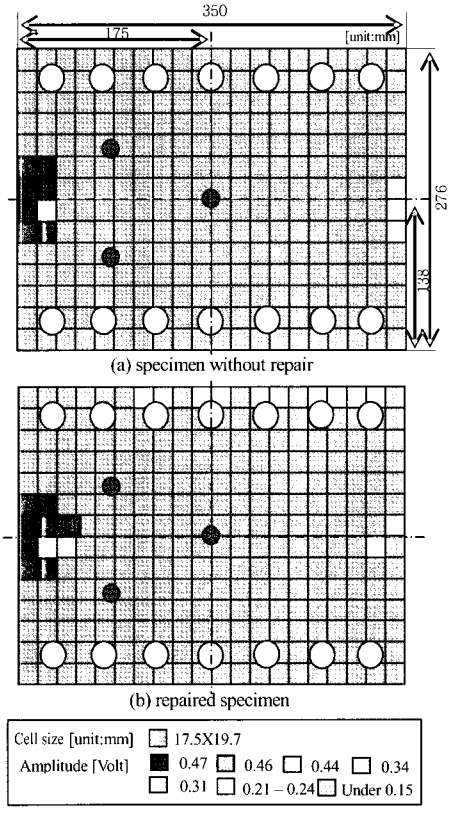

(a) specimen without repair

(b) repaired specimen

Fig. 12 Amplitude profile of delaminations by pitch-catch bond testing

without repair. As shown in the figure, each cell (17.5 mm × 19.7 mm) presents the value of amplitude in volts representing the existence of delamination. A voltage value recorded under 0.15 volt in the APD indicates that there is no delamination according to the comparison to the reference standard. Because the Lamb waves are attenuated by coupling with well-bonded laminates, such good bond signals have low voltage characteristics. On the contrary, an APD voltage value recorded over 0.40 volt was verified by the DPD results and SEM micrographs that there are multiple delaminations and voids. In a disbond region, theoretically the waves travel in the specimen with very little attenuation. As a result, those signals have higher voltage characteristics. After speculation of these results obtained from the APD, it was assumed that LHCLC could cause CFRP laminates to involve higher energy multi-delaminations. When analyzing APD patterns in voltage value, relatively monotonous APD patterns obtained from the specimen without repair appeared in the diagram while varied APD patterns obtained from the repaired specimen appeared. Such results coincide with the general principle that the reliability of CFRP fabrication cured by autoclave is higher than those of repair methods, i.e. the hot-bonding and the cold-bonding used in this experiment. In the meanwhile, it can be also assumed that the low amplitude values obtained from the slightly extended area around the bolt holes for the mount bolts being installed in the fatigue loading machine indicate that cumulative delaminations occurred mainly due to the two-fold cyclic loading.

A method for determining the depth of delaminations in the specimens is presented. The DPD obtained from both the front and the back side located the accurate delamination depth via pulse-echo ultrasonic testing. After the calibration using the reference standard, each peak signal of horizontal full width (HFW) on CRT screen caused by simulated teflon tapes inserted in the reference standard was marked on the screen as an index point so that the peak signals from the specimen can be indicative of the DPD from the specimen. As shown in Fig. 13 and Fig. 14, each cell (5 mm × 5 mm) presents the delamination depth. In order to investigate the accuracy of the DPD, a scanning method applied on front and back sides of the specimen was performed. The reason why the DPD obtained from the front and the back side are different is the reflection of the ultrasound beam at the matrix interface, i.e. between delaminated laminae, due to the difference of acoustic impedance. When analyzing the DPD obtained from the specimen without repair, it is close to the surface where three depth located delaminations occurred at the heat-affected area while it is in the middle of the cross-section where two depth located delaminations occurred at the cyclic-loading only

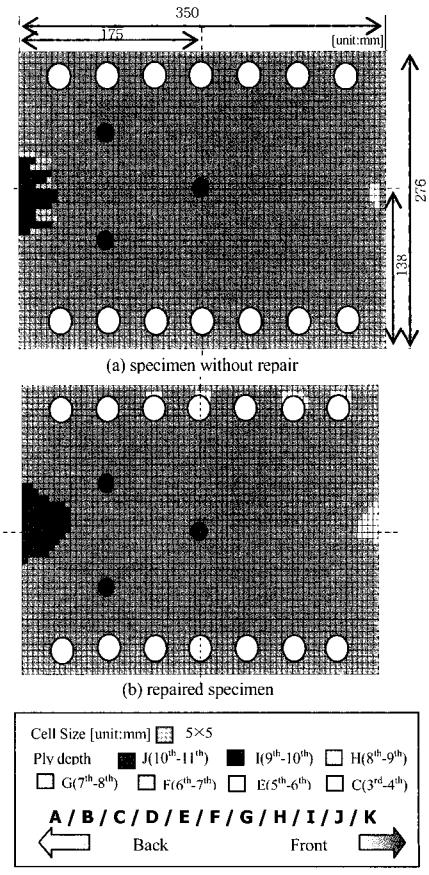

Fig. 13 Depth profile of delaminations by pulse-echo ultrasonics (scanned on front side)

area as shown in the Fig. 13(a). It was also found that there were delicate differences in DPD between Fig. 13(a) and (b) considering the whole area of the cells representing DPD and its characteristics. That is, the delaminated area in the repaired specimen is bigger and the delaminations at cold-bonding repaired area mostly occurred just below the surface of the specimen than those of the specimen without repair. With such results it could be summarized that the localized heating mainly caused subsurface delaminations to occur.

When analyzing DPD obtained from the back side as shown in Fig. 14, the DPD is evenly distributed over the cross section. At the heat affected area delaminations occurred in the multiple depth while the DPD mainly caused by cyclic loading only indicates the patterns similar to those obtained from the front side. In terms of the extent of DPD, the DPD obtained from the repaired specimen is more dispersed than those obtained from the specimen without repair. In addition, it was found that the DPD obtained from the local area repaired by a cold-bonding technique indicates that more multiple delaminations were generated. Considering these results, it was summarized that the localized heating mainly caused multiple delaminations to occur over the cross section.

After the results obtained from both the APD and the DPD for the specimen before and after repair, SEM micrography was performed to investigate the effect of the adhesive strength of the fiber-matrix interface under the localized heating and cyclic loading combined. Fig. 15 shows normal area after two-fold cyclic loading and localized heating. In Fig. 16 and Fig. 17, both SEM micrographs represent the existence of delaminations. It should be noted with a careful attention to the differences between Fig. 16 and Fig. 17. In Fig. 16(b), the evidence of strong adhesive strength between delaminated laminae can be seen. On the other hand, Fig. 17(b) indicates a clear existence of little adhesive strength between delaminated laminae.

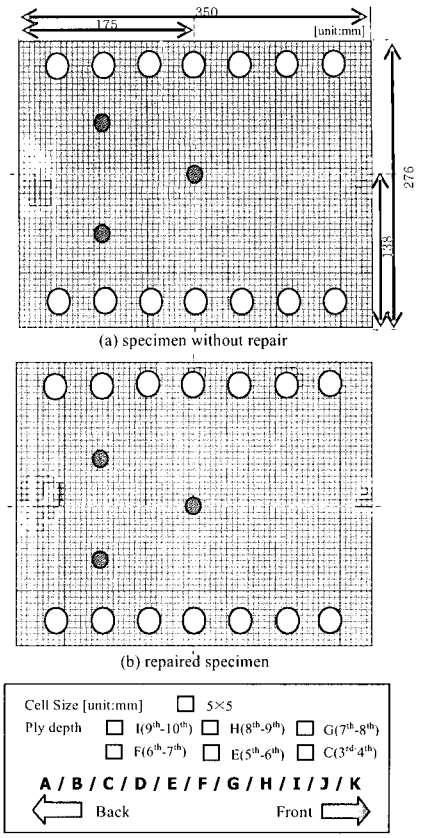

Fig. 14 Depth profile of delaminations by pulse-echo ultrasonics (scanned on back side)

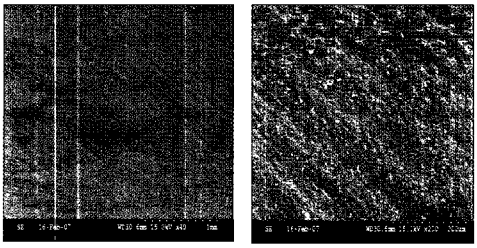

(a) × 40 (b) × 200

Fig. 15 SEM micrographs of normal area after two-fold cyclic loading and localized heating

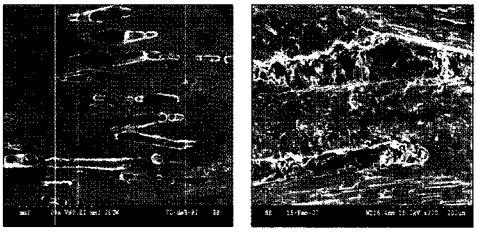

(a) × 40 (b) × 200

Fig. 16 SEM micrographs of delaminations in the localized heating area (specimen without repair)

Consequently, the results showed that how multiple delaminations in depth in the composite laminates could be affected by the strength of the adhesive bonding between laminae.

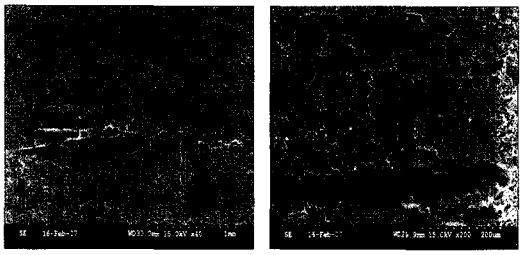

(a) × 40 (b) × 200

Fig. 17 SEM micrographs of delaminations in the localized heating area (repaired specimen)

The results of the AE signal analysis obtained by the two different conditions, i.e. (1) the LHCLC and (2) the CLO, showed different characteristic patterns. As a calibration procedure, a pencil lead was broken at a convenient location with respect to the sensor so that the processed pulse can be analyzed for amplitude, counts, and energy, and these parameters were selected for the reference. Such parameters obtained from the specimen were compared to the reference level, i.e. threshold level, for screening and analysis purposes. Frequency spectra based on the dominant frequencies and cumulative AE events comprised of ringdown counts were mainly correlated with the physical phenomena happened during the localized heating. For the period of the CLO, on the contrary, most frequencies obtained from the specimen were recorded under 100 kHz that is out of bandwidth in this experimental set-up. Moreover, most AE events occurred very intensively only when the specimen was getting heat stress during the LHCLC. In summation, because the attenuation of AE can be relatively high in composites due to absorption of sound energy by the matrix, high frequency components obtained during the CLO may be selectively absorbed by the matrix and scattered by filaments. In addition, because the threshold and gain were adjusted to obtain a practical reference level, such a sound energy may fail to raise the threshold and ringdown count.

The power spectra pattern shown in Fig. 18 show the typical characteristics of main frequencies obtained during the LHCLC for the specimen before and after repair. It was found

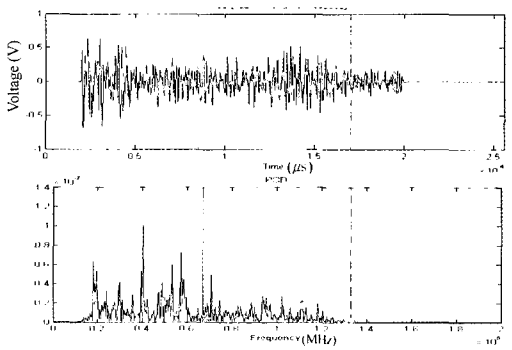

(a) specimen without repair

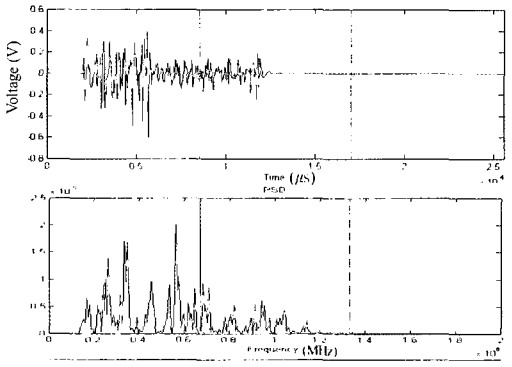

(b) repaired specimen

Fig. 18 AE signals from delaminations mainly due to thermal stress at a heating cycle

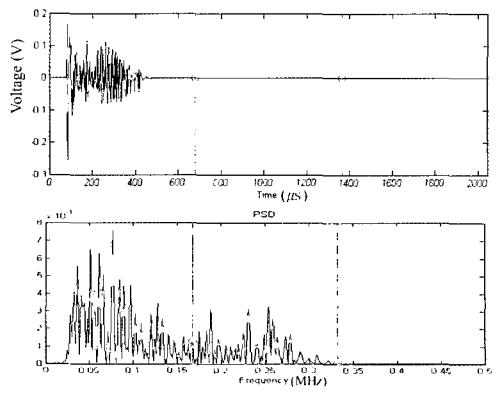

Fig. 19 Typical noise signals due to thermal stress

that the majority of high amplitude signals were at frequencies between 100 kHz and 500 kHz. On the contrary, Fig. 19 represents the typical characteristics of noise signals obtained during the CLO. It was also found that the majority of low amplitude signals were at frequencies less than 50 kHz. In conclusion, most events accompanying main frequencies between 100 kHz and 500 kHz happened at several different LHCLC stages while AE events due to CLO appeared negligible over the whole period.

Fig. 20 shows the relationship between the cumulative number of AE events and temperature gradient at each LHCLC stage. The number of AE events gradually increased at the first stage for both specimen without repair and repaired specimen due to the initial resistance in the laminates to mechanical load. The AE events in turn reached its peak at the third stage and drastically decreased over the latter stages. There

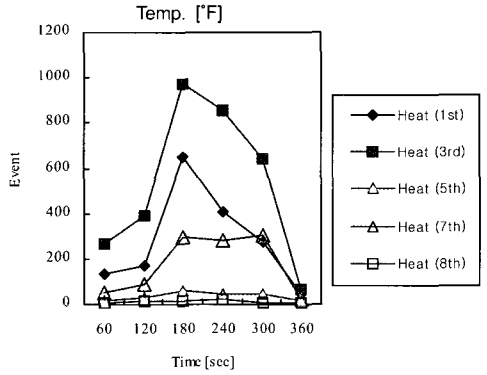

(a) specimen without repair

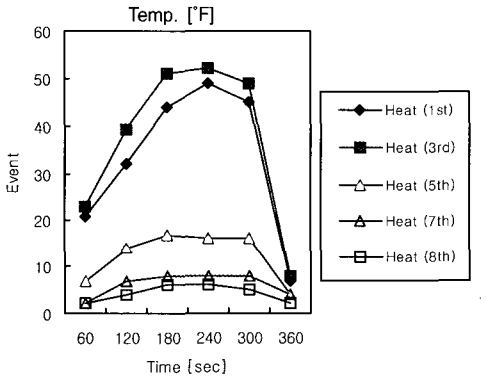

(b) repaired specimen

Fig. 20 AE events with heating cycles

are also noticeable differences in AE events by heating between the repaired specimen and the specimen without repair. First, the number of AE events of the specimen without repair was substantially higher than repaired specimen's. Because the total number of events is a good indication of AE energy, the rate at which the events occur can be indicative of the extent of tructural degradation. Consequently, it is speculated that the specimen lost its retained matrix ductility, hence its ability to resist delamination growth as AE energy releases from the specimen. Secondly, the occurrence of AE events from the repaired specimen was concentrated at the early stage while AE events from the specimen without repair were relatively distributed throughout the stages. After analysis of these results, it was concluded that such composite laminates repaired by cold-bonding technique could be weakened at a relatively early stage by the localized heating.

4. Conclusions

The reliability of cold-bonding repair of CFRP laminates has been monitored for the two conditions, namely the localized heating and cyclic loading combined and the cyclic loading only, by AE testing and further confirmed by pitch-catch low-frequency bond testing, pulse-echo high-frequency ultrasonic testing, and SEM observations. The conclusions are summarized as follows:

1) Delaminations caused by the cyclic loading and localized heating combined could occur in multiple layers while delaminations caused by the cyclic loading only could occur in a few layers.
2) The detectable AE events increased drastically at early stage of local heating cycles while AE events due to cyclic loading only appeared negligible, which indicated composite laminates repaired by cold-bonding could be weakened at a relatively early stage.

3) AE monitoring appeared to be an effective and reliable tool to monitor the integrity of temporarily repaired CFRP laminates in terms of SHM philosophy.

References

BAC5337 (2000) *Boeing Process Spec.: Application of Nonstructural Wet Lay-Up Plies to Composite Panels*

BAC5578 (2002) *Boeing Process Spec.: Manufacture of Advanced Carbon Fiber Reinforced Advanced Composite Structure with Toughened Epoxy Systems, + 350 F Cure*

BAC5980 (2002) *Boeing Process Spec.: Nondestructive Inspection of Composite Parts and Structures*

Boeing SRM (2007) *Structural Repair Manual for B777-200*, D634W201

Bolotin, V. V. (1996) Delaminations in Composite Structures: Its Origin, Buckling, Growth and Stability, Composites Structure, pp. 129-145

Fitch, C. E., Jr. (1991) Pulsed Low Frequency Ultrasonic Bond and Thickness Testing, *Air Transport Association NDT Forum*

Galella, D. (2006) FAA Inspection Research Activities for Composite Materials, *The 2006 Composite Damage Tolerance & Maintenance Workshop*

Hall, S. R. and Conquest, T. J. (1999) The Total Data Integrity Initiative - Structural Health Monitoring; The Next Generation, *Proc. the USAF ASIP,* 2nd Ed.

Kessler, S. S., Spearing S. M., Atalla, M. J., Cesnik, C. E. S. and Soutis, C. (2001) Structural Health Monitoring in Composite Materials Using Frequency Response Methods, accepted for publication by Composites - Part B

Kessler, S. S. (2002) Piezoelectric-Based In-Situ Damage Detection of Composite Materials for Structural Health Monitoring Systems, Ph. D. Thesis, Massachusetts Institute of Technology

Kim, Sung-Jin, Kwon, Oh-Yang and Jang, Yong-Joon Fatigue Crack Growth Behavior of and Recognition of AE Signals from Composite Patch-Repaired Aluminum Panel, J. KSNT, Vol. 27, No. 1, pp. 48-57

Marantidis C., Van Way, C. B. and Kudva, J. N. (1994) Acoustic Emission Sensing in an On-Board Smart Structural Health Monitoring System for Military Aircraft, *Proc. the SPIE Conference on Smart Structures and Integrated Systems*, Vol. 2191, pp. 258-264

Matsuzaki, R. and Todoroki, A. (2006) Wireless Detection of Internal Delamination Cracks in CFRP Laminates Using Oscillating Frequency Changes, Composites Science and Technology, Vol. 66, pp. 407-416

Matt, H. M. (2006) Structural Diagnostics of CFRP Composite Aircraft Components by Ultrasonic Guided Waves and Built-In Piezoelectric Transducers, U. of California, pp. 35-43

MIL-HDBK-17 (1999) *Guidelines for Characterization of Structural Materials*, Vol. 1, The Composite Materials, U.S. Department of Defense

Teller, C., Dierks, K., Bar-Cohen, Y., and Shaw, N. (1987) Nondestructive Evaluation of Adhesive Bonds, *Proc. 16th Symposium on Nondestructive Evaluation*, San Antonio, Texas

Worlton, D. C. (1961) Experimental Confirmation of Lamb Waves at Megacycle Frequencies, J. of Applied Physics, Vol. 32, pp. 967-971